



## Preparation and Photodynamic Properties of Methylene Blue-Silica Nanospheres

Heyong Huang, Yan Ding, Jiahong Zhou and Yuying Feng\*

Analysis and Testing Center, Nanjing Normal University, Nanjing 210023, PRC

### ABSTRACT

*This article presents the development and characterization of SiO<sub>2</sub> nanoparticles loaded with methylene blue (SiO<sub>2</sub>-MB), which are designed to administered for photodynamic therapy (PDT). Induced by light irradiation, the entrapped MB generated <sup>1</sup>O<sub>2</sub>, and the produced <sup>1</sup>O<sub>2</sub> was measured with anthracene-9,10-dipropionic acid. In comparison to the unmodified MB, the MB nanoparticles display lower singlet oxygen production but higher DNA photocleavage capability. Furthermore, in vitro experiments illustrated that SiO<sub>2</sub>-MB was efficiently taken up by tumor cells, and that light irradiation of such impregnated cells resulted in significant cell death. Thus, these properties of SiO<sub>2</sub>-MB could possibly make it especially promising for use in clinical photodynamic therapy.*

**Keywords:** Nanomaterials; Methylene blue; Silica dioxide; Photodynamic therapy

### INTRODUCTION

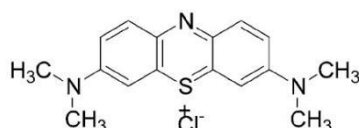
Photodynamic therapy (PDT) has emerged as a promising method for overcoming some of the inherent problems in classical cancer therapies [1-5]. It involves the selective delivery of photosensitizers (PS), such as Photofrin, to tumors. When excited with an appropriate wavelength of visible or near-infrared light, the PS produces singlet oxygen (<sup>1</sup>O<sub>2</sub>) and other reactive oxygen species, resulting in irreversible damage to tumor cells, with minimal systemic toxicity.

An ideal photosensitizer should satisfy several criteria: chemical purity, tumor selectivity, minimal dark toxicity, rapid systemic clearance, high photochemical reactivity and activation at longer wavelengths [4]. Currently available photosensitizers only partially fulfill these criteria. Many new PDT agents have been investigated including chlorins and phthalocyanines, with favorable PDT properties. Methylene blue, a water-soluble phenothiazine derivative, has been used for a variety of clinical applications, including PDT [4,6]. Methylene blue is approved by the FDA for use in methemoglobinemia. The high quantum yield of <sup>1</sup>O<sub>2</sub> generation ( $\Phi\Delta \sim 0.5$ ) [7], coupled with relatively low dark toxicity, makes methylene blue an attractive candidate for PDT. However, clinical use of methylene blue for PDT has been limited because of lack of significant therapeutic efficacy following systemic administration. Methylene blue accumulates extensively in erythrocytes [8] and endothelial cells [9,10], where it is reduced to leucomethylene blue, resulting in the loss of photodynamic activity[11]. Unfortunately, little

investigation has been conducted using drug delivery carriers with MB (Chart 1), although there has been much effort focused on the synthesis or modification of MB [11-14].

In recent years, nanoparticles have received increasing attention as a possible means of delivering PDT agents [15,16]. The porous hollow silica nanoparticle (SN), a new drug carrier for photosensitive drugs, has been receiving quickly increased research attentions because of its water-solubility, high stability, immunity to microbial attack and compatibility with biological systems, which is obviously superior to conventional drug delivery systems. In addition, a pronounced advantage of this new type of carrier is that it will never release PS but allow active oxygen species to diffuse out through the micro-holes within the shell part of SNs. Therefore, this kind of carrier seems to meet the request for PDT very well.

In this paper, MB encapsulated in silica nanoparticles have been successfully prepared through the sol-gel method. The photocleavage capability to DNA improved effectively. In addition, the singlet oxygen production and PDT efficacy to cancer cell *in vitro* was discussed (Scheme 1).



**Scheme 1: Structure of methylene blue (MB)**

## MATERIALS AND METHODS

### Reagents

9,10-Anthracendipropionic acid, ethidium bromide (EB), dimethyl sulfoxide (DMSO), Methylene Blue (MB), tetraethylorthosilicate (TEOS), and calf thymus deoxyribonucleic acid (CT-DNA) were all purchased from Sigma-Aldrich Corporation. Dulbecco's minimum essential medium (DMEM) was from Gibco. 3-(4,5-dimethylthiazol-2-yl)2,5-diphenyl tetrazolium bromide (MTT) was from Amosco.

### Preparation and Characterization of MBNP

The sol-gel silica nanoparticles were made via a modified method [17-19]. The typical reaction solution consists of 24 mL methanol, 6 mL ammonium hydroxide (30% wt of ammonia) and 80  $\mu$ L MB solution (20 mg/mL). On mixing the solution by vigorous magnetic stirring, 0.2 mL TEOS was added dropwise to initiate the hydrolysis reaction. The resulting solution was stirred at room temperature for approximately 2 h before it was transferred to the Amicon ultrafiltration cell, where it was rinsed rigorously with distilled water and ethanol to ensure removal of all unreacted reactants. The particle suspension was finally passed through the suction filtration system with a 0.02  $\mu$ m filter membrane and dried to yield an end product of MBNP.

### Characterization of MBSN

Transmission electron microscopy (TEM) image was obtained on a JEM-1200EX II electron microscopy with an acceleration voltage of 200 kV. A VARIAN CARY 5000 UV-visible recording spectrophotometer was used for absorption measurements. Fluorescence spectra were measured by a Perkin-Elmer LS-50B fluorometer with an excitation wavelength of 480 nm.

### Singlet Oxygen Detection

Singlet oxygen detection measurements were carried out in a plastic cuvette using the disodium salt of 9,10-anthracendipropionic acid (ADPA) as a singlet oxygen sensor [20]. In a typical experiment, an aqueous solution of ADPA (150 mL, 5.5 mmol) was mixed with MBNP (3 mL). The control experiment used ADPA mixed with aqueous solution of MB, which MBs been prepared by adding small amounts of concentrated DMSO solutions of MB to phospMBte buffer. These solutions were irradiated with a 500 W high-voltage mercury lamp with 470 nm cutoff filter. The optical densities at 378 nm (characteristic absorption peak of ADPA) were recorded every 2 min using VARIAN Cary 5000 UV-vis spectrophotometer.

### Photodegradation of CT DNA Analysis

To study the PDT properties of MBNP, the air-saturated buffer solution of CT DNA (8 mmol/L) (10 mmol/L ammonium acetate, 100 mmol/L sodium chloride, pH=7.0 containing ethidium bromide (16 mmol/L) was used as phototherapeutic target, after adding MBSN (MB) into the above solution, the mixture was irradiated with light above 470 nm, and the fluorescence spectrum of the mixture was recorded every 5 min.

#### Photodynamic Effects with Tumor Cells *in vitro*

For studying *in vitro* photodynamic efficiency, 96-well plates were inoculated with cells at  $1 \times 10^5$  cells mL<sup>-1</sup> density overnight. The medium was removed, the wells were rinsed with sterile PBS, and serum-free medium (100 mL) with MB or SiO<sub>2</sub>-MB was placed into each well. After incubation overnight, the cells were irradiated by light and the percentage of dead cells was evaluated by using the MTT assay.

## RESULTS AND DISCUSSION

#### TEM Imaging of MBNP

A TEM image of SiO<sub>2</sub>-MB prepared by reprecipitation method is shown in Figure 1. The particles are nearly ball-like, having uniform size distribution, with an average diameter of 25 nm.

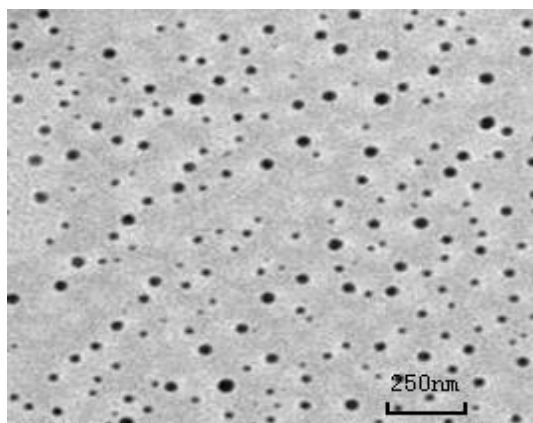
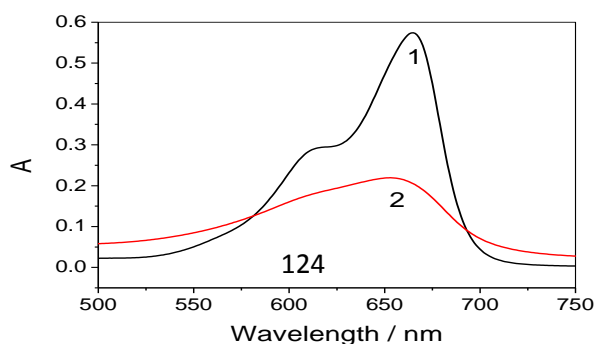


Figure 1: TEM image of SiO<sub>2</sub>-MB

#### Optical Spectroscopy

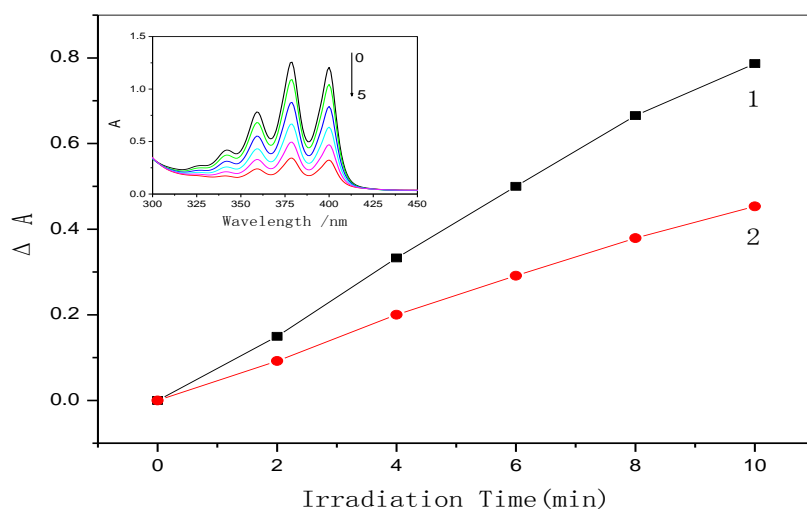
Between 550 nm and 800 nm, free MB has two characteristic absorbance bands, located at 664 nm and 600 nm respectively (Figure 2). After MB was converted into SiO<sub>2</sub>-MB, the intensity of the two absorbance bands decreased. This phenomenon indicated that the surroundings of MB molecules has been changed, i.e., the MB molecules on the surface of nanoparticles can prevent the inner MB molecules from water molecules, and the inner MB molecules exist in the hydrophobic surroundings [21]. Furthermore, the absorption spectrum of two aqueous solutions of MB and SiO<sub>2</sub>-MB has shown a remarkable difference after lifting to stand for three days. The absorption intensity of two characteristic absorbance bands of SiO<sub>2</sub>-MB has no obvious change but that of the MB aqueous solution decreased in intensity. Thus, comparing the changes in the absorption spectrum, it can be determined that SiO<sub>2</sub>-MB has excellent stability in the aqueous solution. This could be due to negative surface charges on SiO<sub>2</sub>-MB.



**Figure 2: Absorption spectra of MB (1) and SiO<sub>2</sub>-MB (2) in the aqueous solution.****Detection of Singlet Oxygen**

Singlet oxygen is believed to be one of the reactive intermediates in PDT. Consequently, the quantum yield of <sup>1</sup>O<sub>2</sub> is an important parameter to evaluate the application potential of the photosensitizer in PDT. Thus, the ADPA bleaching experiment was carried out to detect the <sup>1</sup>O<sub>2</sub> generation quantum yield of SiO<sub>2</sub>-MB and MB. If the absorption intensity of ADPA continuously decreased as the irradiated time increase, the generation of singlet oxygen is confirmed (Figure 3 inset panel). Because <sup>1</sup>O<sub>2</sub> can react irreversibly with ADPA to produce the endoperoxide derivative of ADPA (Scheme 1), and the <sup>1</sup>O<sub>2</sub> generation quantum yield can be calculated through comparing the decrease of the absorption intensity of ADPA [22].

ADPA bleaching experiments showed that the <sup>1</sup>O<sub>2</sub> generation efficiency of SiO<sub>2</sub>-MB is 0.58 (taking free MB as a reference) (Figure 3). The result indicated that the singlet oxygen delivery is hindered by the embedding in this case. This difference in activity may be partially attributed to the microenvironments in the nanoparticles, in particular, the local sequestration of produced <sup>1</sup>O<sub>2</sub> by the matrix. Moreover, as mentioned in the previous section, MB forms dimers in nanoparticles, which do not absorb light at 650 nm to produce <sup>1</sup>O<sub>2</sub>.

**Figure 3: Photosensitized ADPA bleaching by measuring absorbance decrease ( $\Delta A$ ) at 378 nm as a function of irradiation time. (1: MB; 2: SiO<sub>2</sub>-MB) (inset picture: 0–6: Absorption spectra of ADPA in SiO<sub>2</sub>-MB system were irradiated for 0, 2, 4, 6, 8 and 10 min).****Photodegradation of CT-DNA Analysis**

MB were investigated as a potential DNA cleavage agent. According to previous references, MB can abstract one electron from DNA upon irradiation, and thus induce damage and cleavage of DNA. One electron transfer from DNA to triplet MB will result in the formation of two reduced forms of MB, MB<sup>•-</sup> and MBH<sub>2</sub>, which are the precursors of superoxide anion radical (O<sub>2</sub><sup>-</sup>) and hydroxyl radical (<sup>•</sup>-OH). On the other hand, singlet oxygen (<sup>1</sup>O<sub>2</sub>) is formed via the energy transfer from triplet MB to molecular oxygen. These reactive oxygen species promote the cleavage of DNA [23].

When irradiation was carried out in the SiO<sub>2</sub>-MB-EB-CTDNA buffer aerobic solution with light above 470 nm, 47.2% binding sites can be destroyed during 25 min, while only 7.6% binding sites were damaged when free MB was used as the photosensitizer. These results suggest that the photocleavage ability of SiO<sub>2</sub>-MB is superior to free MB (Figure 4).

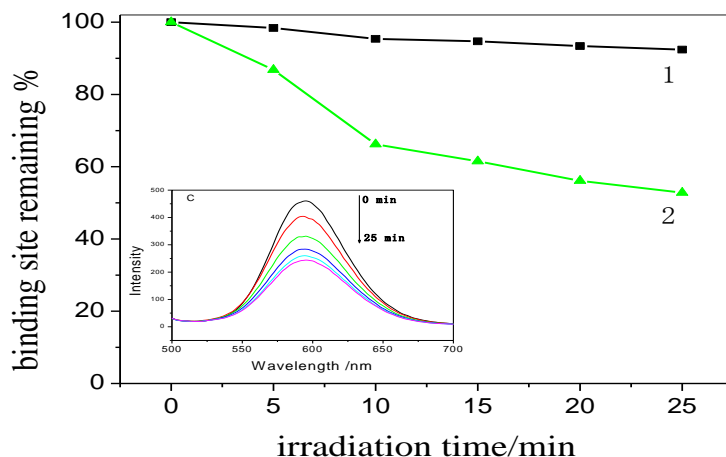


**Figure 4:** Photocleavage percent of CT-DNA by MB (1) or SiO<sub>2</sub>-MB (2) detected by photodegradation percentage of ethidium bromide to the damaged CT-DNA (inset picture: photodegradation of CT-DNA by SiO<sub>2</sub>-MB by irradiated for 0, 5, 10, 15, 20 and 25 min)

### Photodynamic Effects *in vitro*

The *in vitro* results indicate a direct relationship between the dose of drug or light and the photosensitizing efficiency. The results showed that after irradiation, both SiO<sub>2</sub>-MB and MB can cause significant cell death, and such photodynamic activity is dependent on both drug dose (Figure 5A) and light dose (Figure 5B). Comparative studies with SiO<sub>2</sub>-MB and MB demonstrated that the photodynamic activity of SiO<sub>2</sub>-MB was higher than that of the MB under the same experimental conditions, which is possibly because of the difference in their <sup>1</sup>O<sub>2</sub> generation ability. The above results indicated that encapsulation of MB in nanoparticles enhanced the tumor cell kill over the dose range studied.

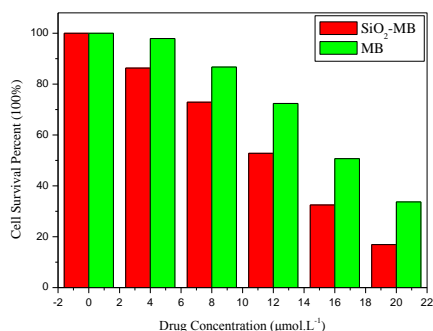


**Figure 5A**

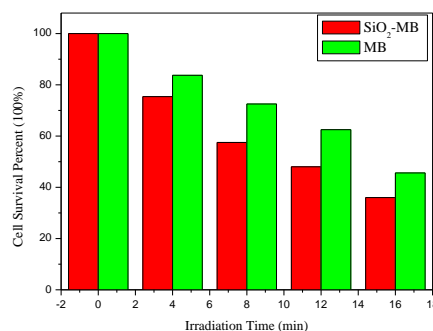


**Figure 5B**

**Figure 5:** A) *In vitro* photosensitizing efficiency of SiO<sub>2</sub>-MB in HeLa cells at different drug concentrations and the same irradiation B) *In vitro* PDT photosensitizing efficiency of SiO<sub>2</sub>-MB with prolonged irradiation time

### CONCLUSION

In conclusion, SiO<sub>2</sub>-MB can be prepared through a simple method greatly improving the water solubility, stability and ability of singlet oxygen generation. Furthermore, the high <sup>1</sup>O<sub>2</sub> generation quantum yield of SiO<sub>2</sub>-MB results in a higher capability to photocleave DNA than free MB, and the *in vitro* photodynamic activity of SiO<sub>2</sub>-MB were much higher than those of MB under the same experimental conditions. The properties of SiO<sub>2</sub>-MB make it a likely prospect for application in the clinical therapy of PDT.

## ACKNOWLEDGMENTS

This work was supported by the Natural Science Foundation of China (GrantNo.20603018) and Science Foundation of Jiangsu (Grant No. BM2007132), China. We gratefully acknowledge the anonymous reviewers whose comments helped to improve the manuscript.

## REFERENCES

- [1] Mac IJ; Dougherty TJ. *J Porphyr Phthalocyanines*. **2001**, 5, 105–129.
- [2] Dougherty TJ; Gomer CJ; Henderson BW. *J Natl*. **1998**, 90, 889–905
- [3] Schuitmaker JJ; Bass P; VanLeengoed H, Meulen FW. *J Photochem Photobiol*. **1996**, 34, 3–12.
- [4] WM Sharman; CM Allen; JE Lier. *Drug Discov Today*.**1999**; 4: 507–517.
- [5] Dolman D; Fukumura D; Jain RK. *Nat Rev Cancer*. **2003**, 3, 380–387.
- [6] Gabrielli D; Belisle E; Severino D; Kowaltowski AJ; Baptista MS. *Photochem Photobiol*. **2004**, 79, 227–232.
- [7] Redmond RW; Gamlin JN. *Photochem Photobiol*. **1999**, 70, 391–475.
- [8] Sass MD; Caruso CJ; Axelrod DR. *J Lab Clin Med*. **1967**, 69, 447–455.
- [9] Bongard RD; Merker MP; Shundo R; Okamoto Y; Roerig DL; Linehan JH; Dawson CA. *J Physiol*. **1999**, 269, 78–84.
- [10] Olson LE; Merker MP; Patel MK; Bongard RD; Daum JM; Johns RA; Dawson CA. *Ann Biomed Eng*. **2000**, 28, 85–93.
- [11] Gabrielli D; Belisle E; Severino D; Kowaltowski AJ; Baptista M. *Photochem Photobiol*. **2004**, 79, 227–232.
- [12] Mellish K J; Cox RD; Vernon DI; Griffiths J; Brown SB. *Photochem Photobiol*. **2002**, 75, 392–397.
- [13] Tuite EM; Kelly JM. *J Photochem Photobiol B*. **1993**, 21, 103–124.
- [14] Wainwright M; Phoenix DA; Rice L; Burrow SM; Waring J. *J Photochem Photobiol B*. **1997**, 40, 233–239.
- [15] Konan YN; Gurny R; Allemann E. *J Photochem Photobiol. B*. **2002**, 66, 89–106.
- [16] Wang SZ; Gao RM; Zhou FM; Selke M. *J Mater Chem*. **2004**;14: 487–493.
- [17] Hao X; Fei Y; Eric E; Kopelman R. *J Biomed Mater Res*. **2003**, 66, 870–879.
- [18] Fink WA; Bohn E. *J Colloid Interface Sci*. **1968**, 26, 62–69.
- [19] Xu H; Aylott JW; Kopelman R; Miller TJ; Philbert MA. *Anal. Chem*. **2001**, 73, 4124–4133.
- [20] Lindig BA; Rodgers MA; Schap AP. *J Am Chem Soc*. **1980**, 102, 5590–5593.
- [21] Zou W; An JY; Jiang LJ. *Acta Biochim Biophys Sin*. **1995**, 6, 685–689.
- [22] Tang W; Xu H; Kopelman R. *Photochem Photobiol*. **2005**, 81, 242–249.
- [23] He YY; Jiang LJ. *Biochim Biophys Acta*. **2000**, 1523, 29–36.